

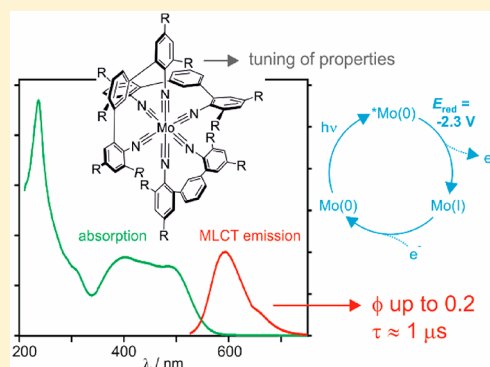
# Long-Lived, Strongly Emissive, and Highly Reducing Excited States in Mo(0) Complexes with Chelating Isocyanides

Patrick Herr,<sup>†</sup> Felix Glaser,<sup>†</sup> Laura A. Büldt,<sup>†</sup> Christopher B. Larsen, and Oliver S. Wenger<sup>\*†</sup>

Department of Chemistry, University of Basel, St. Johannis-Ring 19, 4056 Basel, Switzerland

## S Supporting Information

**ABSTRACT:** Newly discovered tris(diisocyanide)molybdenum(0) complexes are Earth-abundant isoelectronic analogues of the well-known class of  $[\text{Ru}(\alpha\text{-diimine})_3]^{2+}$  compounds with long-lived  $^3\text{MLCT}$  (metal-to-ligand charge transfer) excited states that lead to rich photophysics and photochemistry. Depending on ligand design, luminescence quantum yields up to 0.20 and microsecond excited state lifetimes are achieved in solution at room temperature, both significantly better than those for  $[\text{Ru}(2,2'\text{-bipyridine})_3]^{2+}$ . The excited Mo(0) complexes can induce chemical reactions that are thermodynamically too demanding for common precious metal-based photosensitizers, including the widely employed *fac*- $[\text{Ir}(2\text{-phenylpyridine})_3]$  complex, as demonstrated on a series of light-driven aryl–aryl coupling reactions. The most robust Mo(0) complex exhibits stable photoluminescence and remains photoactive after continuous irradiation exceeding 2 months. Our comprehensive optical spectroscopic and photochemical study shows that Mo(0) complexes with diisocyanide chelate ligands constitute a new family of luminophores and photosensitizers, which is complementary to precious metal-based  $4d^6$  and  $5d^6$  complexes and represents an alternative to nonemissive Fe(II) compounds. This is relevant in the greater context of sustainable photophysics and photochemistry, as well as for possible applications in lighting, sensing, and catalysis.



## INTRODUCTION

The long-lived luminescent metal-to-ligand charge transfer (MLCT) excited states of complexes with precious  $d^6$  metals such as Ru(II), Ir(III), Os(II), or Re(I) form the basis for many photophysical and photochemical applications, for example in luminescent devices,<sup>1</sup> sensing,<sup>2,3</sup> solar energy conversion,<sup>4</sup> and photoredox catalysis.<sup>5</sup> There is a long-standing interest in obtaining complexes with similarly favorable electronic structures made from cheaper first-row transition metal elements.<sup>6–8</sup> Fe(II) is an obvious and much explored target,<sup>9–15</sup> because iron is the most abundant and cheapest transition metal in Earth's crust. However, such  $3d^6$  complexes have energetically low-lying metal-centered (MC) excited states that deactivate the MLCT states very efficiently.<sup>16–18</sup> Different concepts have been explored to lengthen  $^3\text{MLCT}$  lifetimes in Fe(II) complexes, including the optimization of metal coordination geometries,<sup>19–21</sup> the use of push–pull ligand environments,<sup>22,23</sup> and the enhancement of ligand fields with N-heterocyclic<sup>24–27</sup> or mesoionic carbenes.<sup>28</sup> Recently, these efforts culminated in the discovery of two Fe(III) complexes that luminesce from a ligand-to-metal charge transfer (LMCT) excited state<sup>29,30</sup> and an Fe(II) complex with a  $^3\text{MLCT}$  lifetime of 528 ps in solution at room temperature.<sup>31</sup>

Building on early studies of group 6  $d^6$  metal complexes with isocyanide ligands<sup>32,33</sup> and recent reports of luminescent W(0) complexes with monodentate isocyanides,<sup>34,35</sup> we recently

discovered that chelating diisocyanide ligands give access to Cr(0) and Mo(0) complexes with emissive  $^3\text{MLCT}$  excited states.<sup>36</sup> The Cr(0) complex exhibited an excited-state lifetime of 2.2 ns and a luminescence quantum yield of ca.  $10^{-5}$  in tetrahydrofuran (THF) solution at room temperature,<sup>37</sup> while the Mo(0) complex had a  $^3\text{MLCT}$  lifetime of 166 ns and a quantum yield of 0.023 in toluene.<sup>38</sup> Herein, we report how improved ligand design can enhance both of these properties in Mo(0) complexes by an order of magnitude, and it becomes evident that the initially communicated single example is not merely an academic curiosity, but instead tris(diisocyanide)-molybdenum(0) complexes represent a new family of robust  $4d^6$  complexes with very favorable photophysical properties. Moreover, we demonstrate that excitation of these complexes can induce chemical reactions that are thermodynamically too challenging for typical precious metal-based photosensitizers, such as the well-known *fac*- $[\text{Ir}(\text{ppy})_3]$  complex. For this purpose, we investigated base-promoted homolytic aromatic substitution (BHAS) reactions,<sup>39</sup> which were performed in an intramolecular fashion on a series of substrates specifically designed to elucidate the catalytic properties of the Mo(0) complexes.

Our study complements ongoing research on photoactive complexes with other Earth-abundant metal elements such as

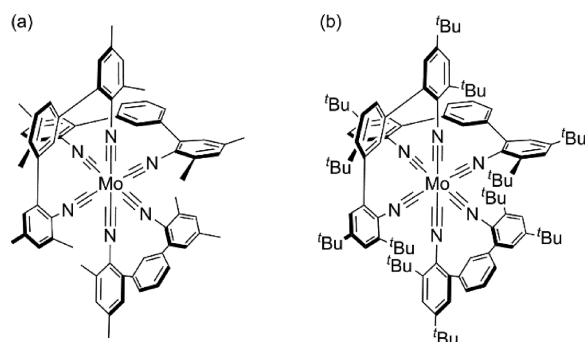
Received: July 11, 2019

Fe,<sup>9–15</sup> Cu,<sup>40–50</sup> Cr,<sup>51–54</sup> Co,<sup>55</sup> Ni,<sup>56–58</sup> Zr,<sup>59,60</sup> W,<sup>34,35,61–63</sup> and Ce,<sup>64</sup> as well as current research on new metal-free organic photosensitizers.<sup>65–69</sup>

## RESULTS AND DISCUSSION

**Synthesis and Infrared Spectroscopy.** Monodentate isocyanide ligands play an important role in organometallic chemistry as alternatives to CO that can be further functionalized,<sup>70,71</sup> and one attractive option is to create polydentate chelating isocyanides.<sup>72–80</sup> In our initial communication, we reported that a *m*-terphenyl backbone is useful to obtain a diisocyanide ligand that binds Mo(0) in chelating fashion, giving access to a homoleptic complex (Scheme 1a,

**Scheme 1.** Molecular Structures of (a)  $[\text{Mo}(\text{L}^{\text{Me}})_3]$  and (b)  $[\text{Mo}(\text{L}^{\text{tBu}})_3]$



$[\text{Mo}(\text{L}^{\text{Me}})_3]$ ) that is structurally and electronically similar to  $[\text{Ru}(\text{bpy})_3]^{2+}$  (bpy = 2,2'-bipyridine).<sup>38</sup> Sterically demanding groups in  $\alpha$ -position to the ligating isocyanides usually stabilize low-valent transition metal species, rendering them less susceptible to electrophilic attack.<sup>71,81</sup> We therefore reasoned that bulkier *tert*-butyl (rather than methyl) substituents could minimize interactions between the Mo(0) center and the solvent, as well as rigidifying the complex, potentially leading to decreased nonradiative <sup>3</sup>MLCT deactivation. In the resulting new  $[\text{Mo}(\text{L}^{\text{tBu}})_3]$  complex (Scheme 1b), this is indeed the case, as our detailed comparative photophysical study with  $[\text{Mo}(\text{L}^{\text{Me}})_3]$  will show. We had previously used  $\text{L}^{\text{tBu}}$  to obtain a luminescent Cr(0) complex,<sup>37</sup> and the synthesis of  $\text{L}^{\text{Me}}$  was reported in our initial Mo(0) communication.<sup>38</sup> The new  $[\text{Mo}(\text{L}^{\text{tBu}})_3]$  complex was prepared by stirring a solution of  $[\text{MoCl}_2(\text{THF})_4]$  and 3 equiv of  $\text{L}^{\text{tBu}}$  in THF over Na/Hg (see Supporting Information page S2 for details). The complex was isolated as a red powder that can be handled under air.

The C≡N stretch frequencies in the free  $\text{L}^{\text{Me}}$  and  $\text{L}^{\text{tBu}}$  ligands are 2113 and 2112  $\text{cm}^{-1}$  (Figure S4), respectively. In the  $[\text{Mo}(\text{L}^{\text{Me}})_3]$  and  $[\text{Mo}(\text{L}^{\text{tBu}})_3]$  complexes, the C≡N vibrations are broad and intense, and their maxima are shifted to 1939 and 1951  $\text{cm}^{-1}$ , respectively, due to  $\pi$ -backbonding.<sup>82</sup>

**Electrochemistry.** In cyclic voltammetry, oxidation of Mo(0) to Mo(I) in deaerated THF with 0.1 M TBAPF<sub>6</sub> results in quasi-reversible waves from which potentials of −0.02 and −0.08 V vs saturated calomel electrode (SCE) can be determined for  $[\text{Mo}(\text{L}^{\text{Me}})_3]$  and  $[\text{Mo}(\text{L}^{\text{tBu}})_3]$ , respectively (Figure 1). These potentials are shifted anodically by 0.2–0.3 V relative to those for previously reported Mo(0) complexes with monodentate arylisocyanides (Table 1).<sup>83</sup>

In principle, this shift could be due to either stabilization of the Mo(0) state or destabilization of the Mo(I) form in the

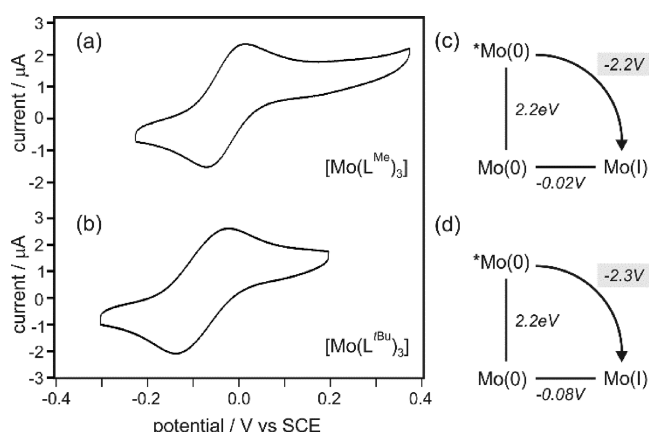


**Figure 1.** Cyclic voltammograms of (a)  $[\text{Mo}(\text{L}^{\text{Me}})_3]$  and (b)  $[\text{Mo}(\text{L}^{\text{tBu}})_3]$  recorded in deaerated THF with 0.1 M TBAPF<sub>6</sub> at 20 °C. The potential scan rates were 0.1 and 0.2 V/s, respectively. The differences in anodic and cathodic peak currents are 86 mV (a) and 116 mV (b). (c, d) Latimer diagrams for  $[\text{Mo}(\text{L}^{\text{Me}})_3]$  and  $[\text{Mo}(\text{L}^{\text{tBu}})_3]$ , based on an energy of 2.2 eV for the emissive <sup>3</sup>MLCT excited state (Figure S7b).

**Table 1.** Electrochemical Potentials (in V vs SCE) in the Electronic Ground State and in the Long-Lived <sup>3</sup>MLCT Excited State

	$E^0 (\text{M}^+/\text{M}^0)$	$E^0 (\text{M}^+/*\text{M}^0)$
$[\text{Mo}(\text{L}^{\text{tBu}})_3]^a$	−0.08	−2.3
$[\text{Mo}(\text{L}^{\text{Me}})_3]^a,b$	−0.02	−2.2
$[\text{Mo}(\text{CN}-\text{C}_6\text{H}_5)_6]^c$	−0.24	
$[\text{Mo}(\text{CN}^{2,6-\text{tPr}}-\text{C}_6\text{H}_3)_6]^c$	−0.32	
<i>fac</i> -[Ir(ppy) <sub>3</sub> ] <sup>d</sup>	0.77	−1.7

<sup>a</sup>This work, measured in THF with 0.1 M TBAPF<sub>6</sub> (Figure 1). <sup>b</sup>From ref 38, measured in THF with 0.1 M TBAPF<sub>6</sub>. <sup>c</sup>From ref 83, measured in THF with 0.1 M TBAPF<sub>6</sub> versus Ag/AgCl. <sup>d</sup>From ref 84.

chelate complexes.<sup>85</sup> It seems likely that the latter effect is dominant, because the bite angle of the chelating  $\text{L}^{\text{Me}}$  and  $\text{L}^{\text{tBu}}$  ligands is expected to become less favorable with increasing oxidation state due to decreasing Mo–C bond distances. Sweeps over greater potential ranges than those in Figure 1 produce lower-quality voltammograms, and ligand reduction was undetectable. However, the observable Mo(0/I) redox wave is the most important one, because it is directly relevant for the photochemistry of  $[\text{Mo}(\text{L}^{\text{Me}})_3]$  and  $[\text{Mo}(\text{L}^{\text{tBu}})_3]$  presented below.

**UV–Vis Absorption, Luminescence, and Transient Absorption Spectroscopy.** The UV–vis spectra of  $[\text{Mo}(\text{L}^{\text{Me}})_3]$  and  $[\text{Mo}(\text{L}^{\text{tBu}})_3]$  exhibit MLCT absorptions between 350 and 550 nm (Figure 2a and b) that cause the orange–red color of these complexes. Ligand-based  $\pi-\pi^*$  transitions appear at shorter wavelengths, and thus the overall spectra are reminiscent of that of isoelectronic  $[\text{Ru}(\text{bpy})_3]^{2+}$ .<sup>36</sup> However, the MLCT absorptions in  $[\text{Mo}(\text{L}^{\text{Me}})_3]$  and  $[\text{Mo}(\text{L}^{\text{tBu}})_3]$  are broader and have higher extinction coefficients by factors of approximately 1.5 and 2.0, respectively.

Upon excitation at 500 nm, both Mo(0) complexes luminesce in deaerated solution at room temperature (Figure 2c and d). The emission is broad and unstructured, and there is a sizable red shift of the emission band maximum when increasing the solvent polarity from *n*-hexane to toluene and THF (540  $\text{cm}^{-1}$  in total for  $[\text{Mo}(\text{L}^{\text{Me}})_3]$  and 410  $\text{cm}^{-1}$  for  $[\text{Mo}(\text{L}^{\text{tBu}})_3]$ ). These observations are compatible with MLCT

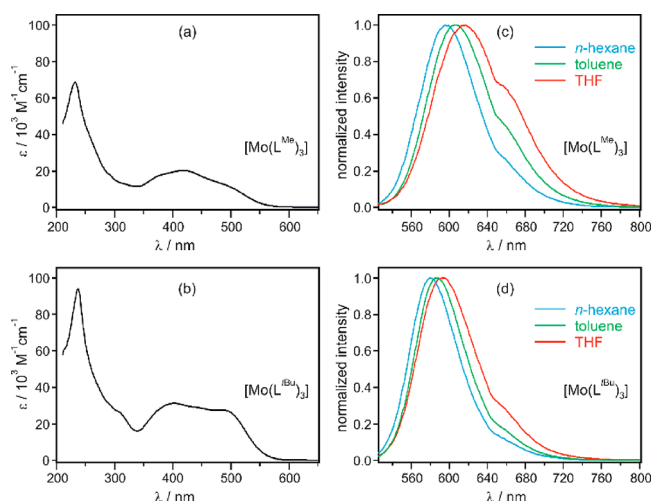


**Figure 2.** UV-vis absorption spectra of (a)  $[\text{Mo}(\text{L}^{\text{Me}})_3]$  and (b)  $[\text{Mo}(\text{L}^{\text{tBu}})_3]$  in THF at 20 °C. Normalized photoluminescence spectra of (c)  $[\text{Mo}(\text{L}^{\text{Me}})_3]$  and (d)  $[\text{Mo}(\text{L}^{\text{tBu}})_3]$  in deaerated solvents at 20 °C. Excitation occurred at 500 nm.

emission, in analogy to  $[\text{Ru}(\text{bpy})_3]^{2+}$ . A key finding is that the luminescence quantum yield ( $\phi$ ) of the  $[\text{Mo}(\text{L}^{\text{tBu}})_3]$  complex is much higher than that of  $[\text{Mo}(\text{L}^{\text{Me}})_3]$  in all investigated solvents. For example, in deaerated toluene at 20 °C, the complex with the more sterically demanding *tert*-butyl-substituted diisocyanide ligand exhibits  $\phi = 0.203$ , whereas the complex with the methyl substituents only has  $\phi = 0.023$  (Table 2). This shows that the aforementioned design principle, according to which better shielding of the metal center from the chemical environment and enhanced complex rigidity should lead to improved photophysical properties, is indeed successful.  $[\text{Ru}(\text{bpy})_3]^{2+}$  has a luminescence quantum yield of 0.095 under optimized conditions in deaerated  $\text{CH}_3\text{CN}$ , more than a factor of 2 lower than  $[\text{Mo}(\text{L}^{\text{tBu}})_3]$ .<sup>86</sup> Such strong luminescence is remarkable for a  $d^6$  MLCT emitter made from an Earth-abundant transition metal and compares very favorably to most Cu(I) diimine complexes.<sup>43,87–89</sup> The latter represent an extremely well investigated class of compounds for which similar luminescence quantum yields required many optimization attempts.

Time-resolved luminescence and transient UV/vis absorption spectroscopy were used to explore the decay characteristics of the emissive excited states and to confirm their MLCT nature. The transient absorption spectra in Figure 3a and b were averaged over a period of 200 ns immediately after excitation at 532 nm with laser pulses of ca. 10 ns duration. In both cases a negative signal (ground-state bleach) is detected near 500 nm, coincident with the lowest-energy  $^1\text{MLCT}$  absorption bands in Figure 2a and b. Additionally, excited-state absorption bands near 345 nm are observed for both complexes, reminiscent of the absorption bands near 370 nm for  $^3\text{MLCT}$ -excited  $[\text{Ru}(\text{bpy})_3]^{2+}$ , which are caused by  $\pi-\pi^*$

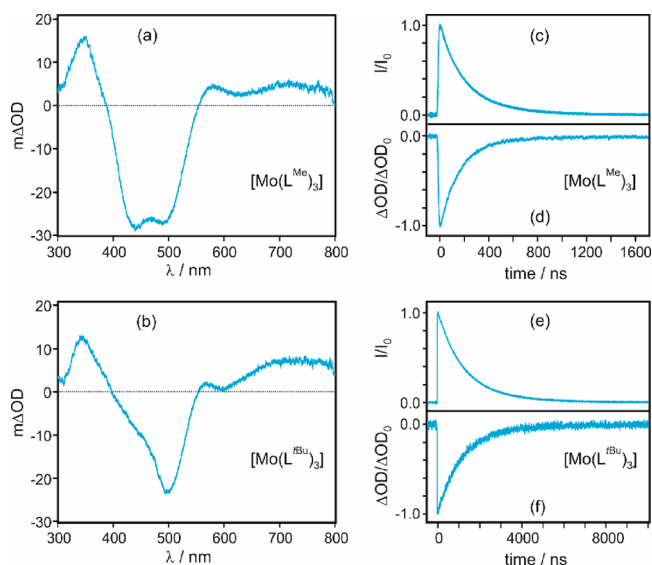


**Figure 3.** Transient absorption spectra measured after excitation of  $10^{-5}$  M solutions of (a)  $[\text{Mo}(\text{L}^{\text{Me}})_3]$  and (b)  $[\text{Mo}(\text{L}^{\text{tBu}})_3]$  in deaerated toluene at 532 nm with laser pulses of  $\sim 10$  ns duration. The signals were time-integrated over 200 ns immediately after excitation. Luminescence decays (c, e) recorded from these solutions at 595/615 nm and recoveries of the MLCT bleaches (d, f) at 485 nm. See Figures S8 and S10 for analogous data recorded in other solvents.

transitions on the transiently reduced bpy ligand.<sup>90</sup> Such short-wavelength excited-state absorption bands combined with ground-state  $^1\text{MLCT}$  bleaches are in fact diagnostic features of MLCT excited states in photoactive Ru(II) and Fe(II) complexes.<sup>22,31</sup>

As expected, the MLCT luminescence at 595/615 nm and the MLCT bleach at 485 nm exhibit the same decay for a given complex (Figure 3c/d and e/f), confirming that the same excited state is monitored by emission and transient absorption spectroscopies. However, the MLCT lifetimes ( $\tau$ ) extractable from these data sets are markedly different for  $[\text{Mo}(\text{L}^{\text{tBu}})_3]$  and  $[\text{Mo}(\text{L}^{\text{Me}})_3]$  in all investigated solvents (Figure S10). For instance, in deaerated toluene at 20 °C,  $\tau = 166$  ns for  $[\text{Mo}(\text{L}^{\text{Me}})_3]$ , while for the  $[\text{Mo}(\text{L}^{\text{tBu}})_3]$  complex, a biexponential decay with  $\tau_1 = 1110$  ns (85%) and  $\tau_2 = 2330$  ns (15%) is observed (Table 2). Thus, the factor-of-10 increase in luminescence quantum yield when going from  $[\text{Mo}(\text{L}^{\text{Me}})_3]$  to  $[\text{Mo}(\text{L}^{\text{tBu}})_3]$  (see earlier) is accompanied by an equivalent increase in excited-state lifetime, compatible with the view that the rate for radiative decay from the emissive MLCT states is similar in both complexes, whereas the rate for nonradiative decay is decreased by an order of magnitude in  $[\text{Mo}(\text{L}^{\text{tBu}})_3]$ . This is additional confirmation for the success of the design concept outlined in the Introduction, and it is evident that the bulkier *tert*-butyl substituents lead to much improved photophysical properties relative to the methyl substituents.

**Table 2.**  $^3\text{MLCT}$  Excited-State Lifetimes ( $\tau$ ) and Luminescence Quantum Yields ( $\phi$ ) in Deaerated Solvents at 20 °C

	<i>n</i> -hexane			toluene			THF		
	$\tau_1$ (ns)	$\tau_2$ (ns)	$\phi$	$\tau_1$ (ns)	$\tau_2$ (ns)	$\phi$	$\tau_1$ (ns)	$\tau_2$ (ns)	$\phi$
$[\text{Mo}(\text{L}^{\text{tBu}})_3]^a$	1040 (76%)	2370 (24%)	0.190	1110 (85%)	2330 (15%)	0.203	610 (73%)	1610 (27%)	0.058
$[\text{Mo}(\text{L}^{\text{Me}})_3]^b$	225 (100%)		0.045	166 (100%)		0.023	74 (100%)		0.006

<sup>a</sup>This work, extracted from the data in Figure S10; determined using  $[\text{Ru}(\text{bpy})_3]^{2+}$  in aerated  $\text{CH}_3\text{CN}$  as standard ( $\phi = 0.018$ ).<sup>86</sup> <sup>b</sup>From ref 38.



In all investigated solvents, the luminescence decays and MLCT bleach recoveries are consistently monoexponential for  $[\text{Mo}(\text{L}^{\text{Me}})_3]$ , while for  $[\text{Mo}(\text{L}^{\text{tBu}})_3]$  biexponential kinetics were observed in all experiments. The biexponential decays are tentatively attributed to the presence of different conformers in the latter. In our previously published crystal structure of  $[\text{Cr}(\text{L}^{\text{tBu}})_3]$ , the three  $\text{L}^{\text{tBu}}$  ligands are not equivalent,<sup>37</sup> and interconversion between different conformations seems to be sterically hindered by the *tert*-butyl substituents. In  $[\text{Mo}(\text{L}^{\text{Me}})_3]$ , the methyl substituents impose less hindrance, and interconversion between different conformers can therefore occur on a faster time scale, leading to single-exponential MLCT decays. Related dynamic interconversions have been observed for some  $\text{Ru}(\text{II})$  complexes.<sup>91</sup>

Going from toluene to THF, the MLCT lifetimes and luminescence quantum yields decrease in parallel in both complexes (Table 2). Qualitatively, this can be understood in the framework of the energy gap law,<sup>92</sup> because the MLCT state is energetically stabilized in more-polar THF (red shifts observable in Figure 2c and d), leading to a smaller energy gap to the ground state and consequent faster nonradiative relaxation. Different propensities for energy dissipation via molecular vibrations of the various solvents could further contribute to the observable lifetime and quantum yield changes between *n*-hexane, toluene, and THF. It is likely that the solvent nucleophilicity also plays a role with respect to the excited-state lifetime, especially for  $[\text{Mo}(\text{L}^{\text{Me}})_3]$ , with more nucleophilic solvents more efficiently deactivating the excited state. However, nucleophilicity and energy-gap law effects are difficult to disentangle in low-polarity solvents. The MLCT lifetimes of both complexes are strongly oxygen-sensitive, confirming the triplet nature of these excited states.

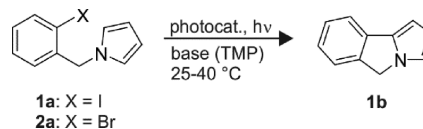
For the photoredox investigations below, the excited-state oxidation potential ( $E_{\text{ox}}^*$ ) is relevant, and this in turn requires knowledge of the energy of the photoactive <sup>3</sup>MLCT state. Therefore, in addition to the emission experiments reported earlier, luminescence spectra were measured at 77 K (Figure S7) to estimate the energy of the electronic origin ( $E_{00}$ ) of the <sup>3</sup>MLCT emission more accurately. This procedure yields an  $E_{00}$  value of 2.2 eV for both complexes, leading to excited-state oxidation potentials of −2.2 and −2.3 V vs SCE for  $[\text{Mo}(\text{L}^{\text{Me}})_3]$  and  $[\text{Mo}(\text{L}^{\text{tBu}})_3]$ , respectively, as indicated in Figure 1c and d (gray shaded areas). Thus, both complexes should be far stronger photoreductants than isoelectronic  $[\text{Ru}(\text{bpy})_3]^{2+}$  ( $E_{\text{ox}}^* = -0.9$  V vs SCE) and *fac*- $[\text{Ir}(\text{ppy})_3]$  ( $E_{\text{ox}}^* = -1.73$  V vs SCE).<sup>84</sup>

**Photochemical Studies.** In our preliminary communication we reported that the  $[\text{Mo}(\text{L}^{\text{Me}})_3]$  complex is able to photocatalyze the rearrangement of an acylcyclopropane substrate to a 2,3-dihydrofuran product,<sup>38</sup> but we noticed that the presence of nucleophiles in the reaction mixture caused degradation of the Mo complex over time. We speculated that this degradation is caused by ligation of nucleophiles to the metal center in  $\text{Mo}(\text{I})$  intermediates formed transiently in the course of the photocatalysis reaction cycle; seven-coordinate molybdenum isocyanide complexes are well-known.<sup>93,94</sup> We will now show that in the new  $[\text{Mo}(\text{L}^{\text{tBu}})_3]$  complex this problem no longer persists, presumably because the bulkier *tert*-butyl substituents more efficiently shield the metal from the chemical environment.

The main purpose of the studies below was to explore the photochemical properties of this new family of d<sup>6</sup> MLCT emitters and to test their robustness in the presence of

nucleophiles over extended irradiation times, rather than to develop new photoredox reactions. Toward this end, we concentrated on net redox-neutral cross-coupling between aryl halides and arenes, which can be considered electron-catalyzed reactions.<sup>39</sup> A specific example is the intramolecular reaction between an aryl iodide and pyrrole (Scheme 2). Base-

### Scheme 2. Intramolecular Base-Promoted Homolytic Aromatic Substitution (BHAS) via Photoredox Catalysis



promoted homolytic aromatic substitution (BHAS) reactions of this type have been identified as a viable alternative to Pd- and Rh-based C–C bond formation, but they often require harsh conditions involving high temperatures and strong bases.<sup>95–100</sup> Photochemical approaches to BHAS not relying on UV excitation have been relatively scarce so far.<sup>101–106</sup>

First, we tested the performance of the  $[\text{Mo}(\text{L}^{\text{Me}})_3]$  complex as a photocatalyst for the reaction in Scheme 2, which can be conveniently followed by monitoring the benzylic <sup>1</sup>H NMR resonances of substrate and product (Figure S13). Using 50 mM substrate 1a in deaerated  $\text{C}_6\text{D}_6$ , 2 equiv of 2,2,6,6-tetramethylpiperidine (TMP) as base, and a photocatalyst loading of 5 mol % in a flame-sealed NMR tube at room temperature, 19% of the substrate was converted to product 1b after irradiation at 470 nm with a light-emitting diode (LED) (ca. 14 W; see Supporting Information page S16 for details) for 1 h (Table 3, entry 1). Maximum conversion of 31% was

**Table 3. Performance of  $[\text{Mo}(\text{L}^{\text{Me}})_3]$ ,  $[\text{Mo}(\text{L}^{\text{tBu}})_3]$ , and *fac*- $[\text{Ir}(\text{ppy})_3]$  in the Light-Driven BHAS Reaction of Scheme 2<sup>a</sup>**

entry	substrate	complex	irradiation time/h	conversion/%
1	1a	$[\text{Mo}(\text{L}^{\text{Me}})_3]$	1	19
2	1a	$[\text{Mo}(\text{L}^{\text{Me}})_3]$	18	31
3	1a	$[\text{Mo}(\text{L}^{\text{tBu}})_3]$	1	100
4	1a	<i>fac</i> - $[\text{Ir}(\text{ppy})_3]$	1	4
5	2a	$[\text{Mo}(\text{L}^{\text{tBu}})_3]$	18	7

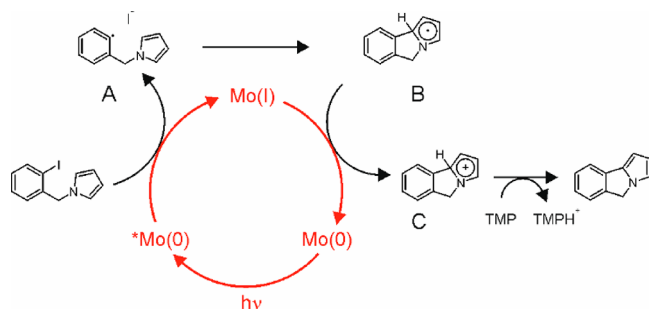
<sup>a</sup>Conditions: 50 mM substrate, 5 mol % metal complex, and 2 equiv of 2,2,6,6-tetramethylpiperidine (TMP) in deaerated  $\text{C}_6\text{D}_6$  at ca. 40 °C. Irradiation at 470 nm with 14 W LED. See Supporting Information pages S16–S19.

observed after 18 h (Table 3, entry 2; Figure S13). Catalyst-based luminescence could not be detected after this time, implying decomposition of  $[\text{Mo}(\text{L}^{\text{Me}})_3]$ . The new  $[\text{Mo}(\text{L}^{\text{tBu}})_3]$  complex, however, catalyzed the reaction to completion within 1 h (Table 3, entry 3; Figure S14). In comparison, use of *fac*- $[\text{Ir}(\text{ppy})_3]$  ( $E_{\text{ox}}^* = -1.73$  V vs SCE) under identical conditions resulted in nearly negligible conversion over the same time period (Table 3, entry 4; Figure S15), and reactions did not reach conclusion even after >100 h of continuous irradiation. As *fac*- $[\text{Ir}(\text{ppy})_3]$  absorbs weakly at wavelengths longer than 450 nm and may therefore create a biased comparison, the experiments with *fac*- $[\text{Ir}(\text{ppy})_3]$  were repeated under 405 nm irradiation, which showed little difference to the results obtained with 470 nm irradiation (Figure S16).

The photochemical BHAS reaction is initiated by a reductive dehalogenation step (see below), and the promising results observed above for  $[\text{Mo}(\text{L}^{\text{tBu}})_3]$  encouraged us to explore the reaction of Scheme 2 with a bromo-substituted substrate (2a), which is more difficult to reduce than the iodoarene of 1a. However, only very modest conversion was observable, and it required extremely long irradiation times (Table 3, entry 5; Figure S17). Over the course of these experiments, we found that the  $[\text{Mo}(\text{L}^{\text{tBu}})_3]$  complex still exhibited stable photoluminescence and was catalytically active after continuous irradiation exceeding 2 months.

A proposed mechanism for the photochemical BHAS reaction with  $[\text{Mo}(\text{L}^{\text{tBu}})_3]$  is presented in Scheme 3. Due to

**Scheme 3. Proposed Mechanism for the Light-Driven Base-Promoted Homolytic Aromatic Substitution (BHAS) Reaction of Scheme 2<sup>a</sup>**



<sup>a</sup>Mo(0), \*Mo(0), and Mo(I) denote the  $[\text{Mo}(\text{L}^{\text{tBu}})_3]$  complex in its initial ground state, its long-lived <sup>3</sup>MLCT-excited state, and its one-electron oxidized form, respectively. TMP is 2,2,6,6-tetramethylpiperidine.

its high reducing power ( $E_{\text{ox}}^* = -2.3$  V vs SCE, Figure 1d), the <sup>3</sup>MLCT-excited Mo(0) complex is able to induce the initial reductive dehalogenation of iodobenzene substrate 1a ( $E_{\text{red}} \approx -2.2$  eV)<sup>107</sup> in an efficient manner. In contrast, the photoexcited *fac*-[Ir(ppy)<sub>3</sub>] complex is substantially less reducing ( $E_{\text{ox}}^* = -1.73$  V vs SCE),<sup>84</sup> and this is likely the main reason for its comparatively poor performance as a catalyst of the reaction in Scheme 2 (Table 3, entry 4). Bromobenzene has a reduction potential of ca.  $-2.4$  V vs SCE (in dimethylformamide (DMF));<sup>107</sup> hence, reductive dehalogenation of substrate 2a becomes inefficient even for photoexcited  $[\text{Mo}(\text{L}^{\text{tBu}})_3]$  (Table 3, entry 5), especially in nonpolar C<sub>6</sub>D<sub>6</sub>. Photodriven reductive dehalogenation reactions are increasingly well-investigated,<sup>108–111</sup> and the general observation is that aryl bromides are substantially more difficult to reduce than aryl iodides,<sup>107,112</sup> and aryl chlorides are even more challenging.<sup>106,113–115</sup> The liberation of I<sup>−</sup> in this initial step (and ligation of I<sup>−</sup> to Mo(I), see earlier)<sup>38</sup> is likely responsible for the rather rapid degradation of  $[\text{Mo}(\text{L}^{\text{Me}})_3]$  and the modest conversion achievable with this first-generation complex (Table 3, entries 1 and 2). Aryl radicals usually have very short lifetimes, but in the specific case of aryl radical A (Scheme 3), intramolecular reaction with the radical interceptor pyrrole to form the cyclic intermediate B is rather efficient.<sup>116</sup> Oxidation of intermediate B by Mo(I) then reinstates the photosensitizer to its initial (electronic ground) state and leads to radical cation C, which can be subsequently deprotonated to afford the final cyclization product. An important difference to thermal BHAS reactions is the

presence of a weak base (TMP) rather than <sup>t</sup>BuOK, and it seems plausible that this renders deprotonation of intermediate B inefficient, making oxidation of B to C necessary before the proton can be abstracted by TMP. With <sup>t</sup>BuOK the reverse order of steps is commonly observed (deprotonation followed by oxidation), and this can give rise to a radical chain mechanism because the radical anion intermediate formed after the deprotonation step is strongly reducing (see Supporting Information page S15 for further details).<sup>100</sup> In the mechanism of Scheme 3, the neutral radical intermediate B is not sufficiently reducing to propagate a radical chain via electron donation to another equivalent of substrate.

To gain further insight into the photochemical performance of  $[\text{Mo}(\text{L}^{\text{tBu}})_3]$ , we explored the carefully selected range of substrates in Table 4, allowing us to probe the influence of

**Table 4. BHAS Reactions To Explore the Photochemical Reactivity of  $[\text{Mo}(\text{L}^{\text{tBu}})_3]$ <sup>a</sup>**

entry	reaction	conversion	duration
1		98%	2h
2		91%	4h
3		93%	145h
4		93%	450h
5		81%	7h

<sup>a</sup>Conditions were similar to those given in Table 3, but using a photoreactor with active cooling to stabilize the temperature of the reaction mixture at 25 °C throughout the complete irradiation process. See Supporting Information pages S16–S21 for details.

structural and electronic variations on the light-driven BHAS reaction in a systematic manner. Substrate 3a differs from 1a by the length of the alkyl linker, and the resulting increased conformational flexibility causes a need for longer reaction times (Table 4, entries 1 and 2; Figure S19). Substrate 4a has the same ethylene linker as 3a, but the reaction time had to be lengthened further from 4 to 145 h to reach a similar level of conversion (Table 4, entry 3; Figure S20). This can be attributed to the fact that *tert*-butylphenyl is a far less efficient interceptor for the aryl radical than pyrrole,<sup>116</sup> rendering the step from A to B in Scheme 3 inefficient. Substrate 5a (Table 4, entry 4) has essentially the same linker length as 4a, but one CH<sub>2</sub> group has been replaced by an O atom. This makes the reaction even slower, now requiring 450 h instead of 145 h (Figure S21). The reason for this is likely the electron-donating nature of the alkoxy linker, rendering the reduction potential of the iodobenzene unit more negative and making reductive deiodination in the initial reaction step more difficult. In substrate 6a (Table 4, entry 5) the alkoxy linker is reversed compared to 5a, with the O atom connected to the *tert*-butylphenyl rather than the iodobenzene unit. This reduces the

necessary reaction time to 7 h (for 81% conversion; Figure S22), likely because the electron-donating nature of the alkoxy linker now mostly acts on the *tert*-butylphenyl unit, making the deiodination of **6a** less difficult and the oxidation step converting intermediate B to C (Scheme 3) more facile. The reactivities observable for the range of substrates **1a–6a** thus seem compatible with the mechanism in Scheme 3. Evidently the  $[\text{Mo}(\text{L}^{\text{tBu}})_3]$  complex is much more robust in these photochemical experiments than  $[\text{Mo}(\text{L}^{\text{Me}})_3]$ , making the new *tert*-butylated complex far superior not just in terms of photophysical properties (see earlier) but also for photochemical applications involving challenging reduction steps not feasible with  $[\text{Ru}(\text{bpy})_3]^{2+}$  or *fac*- $[\text{Ir}(\text{ppy})_3]$ .

## SUMMARY AND CONCLUSIONS

Octahedrally coordinated low-spin  $d^6$  complexes made from precious metals such as Ru, Os, Re, or Ir have attracted interest for more than 40 years, yet to date only a handful of such complexes made from Earth-abundant metals are known to emit from MLCT excited states.<sup>117</sup> Notably, the struggle to identify an MLCT-luminescent Fe(II) complex continues.<sup>11</sup> The present study establishes Mo(0) complexes with chelating diisocyanide ligands as a new family of photoactive compounds that are structurally and electronically closely related to Ru(II) polypyridines. Their photophysical properties can be tuned through ligand modification to a point where their luminescence quantum yield surpasses that achievable for  $[\text{Ru}(\text{bpy})_3]^{2+}$  by more than a factor of 2. Shielding of the metal center from the chemical environment and rigidifying the complex by introducing steric congestion at the ligand periphery is the key to this favorable behavior. In this manner, it has been possible to reduce the rate for nonradiative excited-state decay by more than an order of magnitude between  $[\text{Mo}(\text{L}^{\text{Me}})_3]$  and  $[\text{Mo}(\text{L}^{\text{tBu}})_3]$ , leading to microsecond MLCT lifetimes and luminescence quantum yields as high as 0.203. This design principle furthermore improved the photochemical robustness enormously, making the high reducing power of the <sup>3</sup>MLCT-excited  $[\text{Mo}(\text{L}^{\text{tBu}})_3]$  complex suitable for photochemical transformations that cannot be performed with the widely employed *fac*- $[\text{Ir}(\text{ppy})_3]$  complex. Specifically, the inertness against nucleophilic attack at transiently oxidized Mo(I) metal centers seems of key importance, now permitting photoirradiation over very long periods (days to weeks) without significant complex degradation. A range of base-promoted homolytic aromatic substitution (BHAS) reactions with substrates specifically designed to underpin the photochemical mechanism was explored, demonstrating possibilities and limitations for application of the Mo(0) complexes for these overall redox-neutral reactions involving a thermodynamically challenging reductive dehalogenation and a C–H activation step.

## ASSOCIATED CONTENT

### Supporting Information

The Supporting Information is available free of charge on the ACS Publications website at DOI: 10.1021/jacs.9b07373.

Synthetic protocols, characterization data, additional spectroscopic data, and details regarding photochemical experiments (PDF)

## AUTHOR INFORMATION

### Corresponding Author

\*oliver.wenger@unibas.ch

### ORCID

Oliver S. Wenger: 0000-0002-0739-0553

### Author Contributions

<sup>†</sup>P.H., F.G., and L.A.B. contributed equally.

### Notes

The authors declare no competing financial interest.

## ACKNOWLEDGMENTS

Funding from the Swiss National Science Foundation through Grant no. 200021\_178760 is gratefully acknowledged.

## REFERENCES

- (1) Baldo, M. A.; Thompson, M. E.; Forrest, S. R. High-Efficiency Fluorescent Organic Light-Emitting Devices using a Phosphorescent Sensitizer. *Nature* **2000**, *403*, 750–753.
- (2) Li, A.; Turro, C.; Kodanko, J. J. Ru(II) Polypyridyl Complexes Derived from Tetradentate Ancillary Ligands for Effective Photocaging. *Acc. Chem. Res.* **2018**, *51*, 1415–1421.
- (3) Mari, C.; Pierroz, V.; Ferrari, S.; Gasser, G. Combination of Ru(II) Complexes and Light: New Frontiers in Cancer Therapy. *Chem. Sci.* **2015**, *6*, 2660–2686.
- (4) Hagfeldt, A.; Grätzel, M. Molecular Photovoltaics. *Acc. Chem. Res.* **2000**, *33*, 269–277.
- (5) Yoon, T. P.; Ischay, M. A.; Du, J. N. Visible Light Photocatalysis as a Greener Approach to Photochemical Synthesis. *Nat. Chem.* **2010**, *2*, 527–532.
- (6) Gray, H. B.; Maverick, A. W. Solar Chemistry of Metal-Complexes. *Science* **1981**, *214*, 1201–1205.
- (7) McCusker, J. K. Electronic Structure in the Transition Metal Block and its Implications for Light Harvesting. *Science* **2019**, *363*, 484–488.
- (8) Young, E. R.; Oldacre, A. Iron Hits the Mark. *Science* **2019**, *363*, 225–226.
- (9) Liu, Y. Z.; Persson, P.; Sundström, V.; Wärnmark, K. Fe N-Heterocyclic Carbene Complexes as Promising Photosensitizers. *Acc. Chem. Res.* **2016**, *49*, 1477–1485.
- (10) Duchanois, T.; Liu, L.; Pastore, M.; Monari, A.; Cebrian, C.; Trolez, Y.; Darari, M.; Magra, K.; Frances-Monerris, A.; Domenichini, E.; Beley, M.; Assfeld, X.; Haacke, S.; Gros, P. C. NHC-Based Iron Sensitizers for DSSCs. *Inorganics* **2018**, *6*, 63.
- (11) Wenger, O. S. Is Iron the New Ruthenium? *Chem. - Eur. J.* **2019**, *25*, 6043–6052.
- (12) Steube, J.; Burkhardt, L.; Pöpcke, A.; Moll, J.; Zimmer, P.; Schoch, R.; Wölper, C.; Heinze, K.; Lochbrunner, S.; Bauer, M. Excited-State Kinetics of an Air-Stable Cyclometalated Iron(II) Complex. *Chem. - Eur. J.* **2019**, DOI: 10.1002/chem.201902488.
- (13) Dixon, I. M.; Boissard, G.; Whyte, H.; Alary, F.; Heully, J. L. Computational Estimate of the Photophysical Capabilities of Four Series of Organometallic Iron(II) Complexes. *Inorg. Chem.* **2016**, *55*, 5089–5091.
- (14) Ashley, D. C.; Jakubikova, E. Ironing out the Photochemical and Spin-Crossover Behavior of Fe(II) Coordination Compounds with Computational Chemistry. *Coord. Chem. Rev.* **2017**, *337*, 97–111.
- (15) Zhang, W. K.; Gaffney, K. J. Mechanistic Studies of Photoinduced Spin Crossover and Electron Transfer in Inorganic Complexes. *Acc. Chem. Res.* **2015**, *48*, 1140–1148.
- (16) Carey, M. C.; Adelman, S. L.; McCusker, J. K. Insights into the Excited State Dynamics of Fe(II) Polypyridyl Complexes from Variable-Temperature Ultrafast Spectroscopy. *Chem. Sci.* **2019**, *10*, 134–144.
- (17) McCusker, J. K.; Walda, K. N.; Dunn, R. C.; Simon, J. D.; Magde, D.; Hendrickson, D. N. Subpicosecond <sup>1</sup>MLCT-<sup>5</sup>T<sub>2</sub>



Intersystem Crossing of Low-Spin Polypyridyl Ferrous Complexes. *J. Am. Chem. Soc.* **1993**, *115*, 298–307.

(18) Auböck, G.; Chergui, M. Sub-50-fs Photoinduced Spin Crossover in  $\text{Fe}(\text{bpy})_3^{2+}$ . *Nat. Chem.* **2015**, *7*, 629–633.

(19) Jamula, L. L.; Brown, A. M.; Guo, D.; McCusker, J. K. Synthesis and Characterization of a High-Symmetry Ferrous Polypyridyl Complex: Approaching the  $^5\text{T}_2/{}^3\text{T}_1$  Crossing Point for  $\text{Fe}^{\text{II}}$ . *Inorg. Chem.* **2014**, *53*, 15–17.

(20) Shepard, S. G.; Fatur, S. M.; Rappe, A. K.; Damrauer, N. H. Highly Strained Iron(II) Polypyridines: Exploiting the Quintet Manifold To Extend the Lifetime of MLCT Excited States. *J. Am. Chem. Soc.* **2016**, *138*, 2949–2952.

(21) Fatur, S. M.; Shepard, S. G.; Higgins, R. F.; Shores, M. P.; Damrauer, N. H. A Synthetically Tunable System To Control MLCT Excited-State Lifetimes and Spin States in Iron(II) Polypyridines. *J. Am. Chem. Soc.* **2017**, *139*, 4493–4505.

(22) Mengel, A. K. C.; Förster, C.; Breivogel, A.; Mack, K.; Ochsmann, J. R.; Laquai, F.; Ksenofontov, V.; Heinze, K. A Heteroleptic Push-Pull Substituted Iron(II) Bis(tridentate) Complex with Low-Energy Charge-Transfer States. *Chem. - Eur. J.* **2015**, *21*, 704–714.

(23) Mengel, A. K. C.; Bissinger, C.; Dorn, M.; Back, O.; Förster, C.; Heinze, K. Boosting Vis/NIR Charge-Transfer Absorptions of Iron(II) Complexes by N-Alkylation and N-Deprotonation in the Ligand Backbone. *Chem. - Eur. J.* **2017**, *23*, 7920–7931.

(24) Liu, Y. Z.; Harlang, T.; Canton, S. E.; Chabera, P.; Suarez-Alcantara, K.; Fleckhaus, A.; Vithanage, D. A.; Goransson, E.; Corani, A.; Lomoth, R.; Sundström, V.; Wärnmark, K. Towards Longer-Lived Metal-to-Ligand Charge Transfer States of Iron(II) Complexes: An N-Heterocyclic Carbene Approach. *Chem. Commun.* **2013**, *49*, 6412–6414.

(25) Harlang, T. C. B.; Liu, Y. Z.; Gordivska, O.; Fredin, L. A.; Ponseca, C. S.; Huang, P.; Chabera, P.; Kjaer, K. S.; Mateos, H.; Uhlig, J.; Lomoth, R.; Wallenberg, R.; Styring, S.; Persson, P.; Sundström, V.; Wärnmark, K. Iron Sensitizer Converts Light to Electrons with 92% Yield. *Nat. Chem.* **2015**, *7*, 883–889.

(26) Liu, L.; Duchanois, T.; Etienne, T.; Monari, A.; Beley, M.; Assfeld, X.; Haacke, S.; Gros, P. C. A New Record Excited State  $^3\text{MLCT}$  Lifetime for Metalorganic Iron(II) Complexes. *Phys. Chem. Chem. Phys.* **2016**, *18*, 12550–12556.

(27) Duchanois, T.; Etienne, T.; Beley, M.; Assfeld, X.; Perpete, E. A.; Monari, A.; Gros, P. C. Heteroleptic Pyridyl-Carbene Iron Complexes with Tuneable Electronic Properties. *Eur. J. Inorg. Chem.* **2014**, *2014*, 3747–3753.

(28) Liu, Y. Z.; Kjaer, K. S.; Fredin, L. A.; Chabera, P.; Harlang, T.; Canton, S. E.; Lidin, S.; Zhang, J. X.; Lomoth, R.; Bergquist, K. E.; Persson, P.; Wärnmark, K.; Sundström, V. A Heteroleptic Ferrous Complex with Mesoionic Bis(1,2,3-triazol-5-ylidene) Ligands: Taming the MLCT Excited State of Iron(II). *Chem. - Eur. J.* **2015**, *21*, 3628–3639.

(29) Chábera, P.; Liu, Y.; Prakash, O.; Thyraug, E.; El Nahhas, A.; Honarfar, A.; Essén, S.; Fredin, L. A.; Harlang, T. C. B.; Kjaer, K. S.; Handrup, K.; Ericson, F.; Tatsuno, Y.; Morgan, K.; Schnadt, J.; Häggström, L.; Ericsson, T.; Sobkowiak, A.; Lidin, S.; Huang, P.; Styring, S.; Uhlig, J.; Bendix, J.; Lomoth, R.; Sundström, V.; Persson, P.; Wärnmark, K. A Low-Spin  $\text{Fe}(\text{III})$  Complex with 100-ps Ligand-to-Metal Charge Transfer Photoluminescence. *Nature* **2017**, *543*, 695–699.

(30) Kjaer, K. S.; Kaul, N.; Prakash, O.; Chábera, P.; Rosemann, N. W.; Honarfar, A.; Gordivska, O.; Fredin, L. A.; Bergquist, K. E.; Häggström, L.; Ericsson, T.; Lindh, L.; Yartsev, A.; Styring, S.; Huang, P.; Uhlig, J.; Bendix, J.; Strand, D.; Sundström, V.; Persson, P.; Lomoth, R.; Wärnmark, K. Luminescence and Reactivity of a Charge-Transfer Excited Iron Complex with Nanosecond Lifetime. *Science* **2019**, *363*, 249–253.

(31) Chábera, P.; Kjaer, K. S.; Prakash, O.; Honarfar, A.; Liu, Y. Z.; Fredin, L. A.; Harlang, T. C. B.; Lidin, S.; Uhlig, J.; Sundström, V.; Lomoth, R.; Persson, P.; Wärnmark, K.  $\text{Fe}^{\text{II}}$  Hexa N-Heterocyclic

Carbene Complex with a 528 ps Metal-to-Ligand Charge-Transfer Excited-State Lifetime. *J. Phys. Chem. Lett.* **2018**, *9*, 459–463.

(32) Mann, K. R.; Cimolino, M.; Geoffroy, G. L.; Hammond, G. S.; Orio, A. A.; Albertin, G.; Gray, H. B. Electronic Structures and Spectra of Hexakisphenylisocyanide Complexes of  $\text{Cr}(\text{0})$ ,  $\text{Mo}(\text{0})$ ,  $\text{W}(\text{0})$ ,  $\text{Mn}(\text{I})$ , and  $\text{Mn}(\text{II})$ . *Inorg. Chim. Acta* **1976**, *16*, 97–101.

(33) Mann, K. R.; Gray, H. B.; Hammond, G. S. Excited-State Reactivity Patterns of Hexakisarylsocyno Complexes of Chromium(0), Molybdenum(0), and Tungsten(0). *J. Am. Chem. Soc.* **1977**, *99*, 306–307.

(34) Sattler, W.; Eder, M. E.; Blakemore, J. D.; Rachford, A. A.; LaBeaume, P. J.; Thackeray, J. W.; Cameron, J. F.; Winkler, J. R.; Gray, H. B. Generation of Powerful Tungsten Reductants by Visible Light Excitation. *J. Am. Chem. Soc.* **2013**, *135*, 10614–10617.

(35) Sattler, W.; Henling, L. M.; Winkler, J. R.; Gray, H. B. Bespoke Photoreductants: Tungsten Arylsocyanides. *J. Am. Chem. Soc.* **2015**, *137*, 1198–1205.

(36) Büldt, L. A.; Wenger, O. S. Chromium(0), Molybdenum(0), and Tungsten(0) Isocyanide Complexes as Luminescent and Photosensitizers with Long-Lived Excited States. *Angew. Chem., Int. Ed.* **2017**, *56*, 5676–5682.

(37) Büldt, L. A.; Guo, X.; Vogel, R.; Prescimone, A.; Wenger, O. S. A Tris(diisocyanide)chromium(0) Complex Is a Luminescent Analog of  $\text{Fe}(\text{2,2}'\text{-Bipyridine})_3^{2+}$ . *J. Am. Chem. Soc.* **2017**, *139*, 985–992.

(38) Büldt, L. A.; Guo, X.; Prescimone, A.; Wenger, O. S. A Molybdenum(0) Isocyanide Analogue of  $\text{Ru}(\text{2,2-Bipyridine})_3^{2+}$ : A Strong Reductant for Photoredox Catalysis. *Angew. Chem., Int. Ed.* **2016**, *55*, 11247–11250.

(39) Studer, A.; Curran, D. P. The Electron is a Catalyst. *Nat. Chem.* **2014**, *6*, 765–773.

(40) Hamze, R.; Peltier, J. L.; Sylvinson, D.; Jung, M.; Cardenas, J.; Haiges, R.; Soleilhavoup, M.; Jazzar, R.; Djurovich, P. I.; Bertrand, G.; Thompson, M. E. Eliminating Nonradiative Decay in  $\text{Cu}(\text{I})$  Emitters: > 99% Quantum Efficiency and Microsecond Lifetime. *Science* **2019**, *363*, 601–606.

(41) Gernert, M.; Müller, U.; Haehnel, M.; Pflaum, J.; Steffen, A. A Cyclic Alkyl(amino)carbene as Two-Atom  $\pi$ -Chromophore Leading to the First Phosphorescent Linear  $\text{Cu}^{\text{I}}$  Complexes. *Chem. - Eur. J.* **2017**, *23*, 2206–2216.

(42) Di, D. W.; Romanov, A. S.; Yang, L.; Richter, J. M.; Rivett, J. P. H.; Jones, S.; Thomas, T. H.; Abdi Jalebi, M.; Friend, R. H.; Linnolahti, M.; Bochmann, M.; Credginton, D. High-Performance Light-Emitting Diodes based on Carbene-Metal-Amides. *Science* **2017**, *356*, 159–163.

(43) Leoni, E.; Mohanraj, J.; Holler, M.; Mohankumar, M.; Nierengarten, I.; Monti, F.; Sournia-Saquet, A.; Delavaux-Nicot, B.; Nierengarten, J. F.; Armaroli, N. Heteroleptic Copper(I) Complexes Prepared from Phenanthroline and Bis-Phosphine Ligands: Rationalization of the Photophysical and Electrochemical Properties. *Inorg. Chem.* **2018**, *57*, 15537–15549.

(44) Hossain, A.; Bhattacharyya, A.; Reiser, O. Copper's Rapid Ascent in Visible-Light Photoredox Catalysis. *Science* **2019**, *364*, eaav9713.

(45) Hernandez-Perez, A. C.; Collins, S. K. Heteroleptic Cu-Based Sensitizers in Photoredox Catalysis. *Acc. Chem. Res.* **2016**, *49*, 1557–1565.

(46) Michelet, B.; Deldaele, C.; Kajouji, S.; Moucheron, C.; Evano, G. A General Copper Catalyst for Photoredox Transformations of Organic Halides. *Org. Lett.* **2017**, *19*, 3576–3579.

(47) Nicholls, T. P.; Caporale, C.; Massi, M.; Gardiner, M. G.; Bissember, A. C. Synthesis and Characterisation of Homoleptic 2,9-Diaryl-1,10-Phenanthroline Copper(I) Complexes: Influencing Selectivity in Photoredox-Catalysed Atom-Transfer Radical Addition Reactions. *Dalton Trans* **2019**, *48*, 7290–7301.

(48) Lazorski, M. S.; Castellano, F. N. Advances in the Light Conversion Properties of  $\text{Cu}(\text{I})$ -Based Photosensitizers. *Polyhedron* **2014**, *82*, 57–70.

(49) Czerwieniec, R.; Leitl, M. J.; Homeier, H. H. H.; Yersin, H.  $\text{Cu}(\text{I})$  Complexes - Thermally Activated Delayed Fluorescence.

Photophysical Approach and Material Design. *Coord. Chem. Rev.* **2016**, *325*, 2–28.

(50) Mondal, R.; Lozada, I. B.; Davis, R. L.; Williams, J. A. G.; Herbert, D. E. Exploiting Synergy Between Ligand Design and Counterion Interactions to Boost Room Temperature Phosphorescence from Cu(I) Compounds. *J. Mater. Chem. C* **2019**, *7*, 3772–3778.

(51) Wang, C.; Otto, S.; Dorn, M.; Kreidt, E.; Lebon, J.; Srsan, L.; Di Martino-Fumo, P.; Gerhards, M.; Resch-Genger, U.; Seitz, M.; Heinze, K. Deuterated Molecular Ruby with Record Luminescence Quantum Yield. *Angew. Chem., Int. Ed.* **2018**, *57*, 1112–1116.

(52) Jimenez, J. R.; Doistau, B.; Besnard, C.; Piguet, C. Versatile Heteroleptic Bis-Terdentate Cr(III) Chromophores Displaying Room Temperature Millisecond Excited State Lifetimes. *Chem. Commun.* **2018**, *54*, 13228–13231.

(53) Stevenson, S. M.; Shores, M. P.; Ferreira, E. M. Photooxidizing Chromium Catalysts for Promoting Radical Cation Cycloadditions. *Angew. Chem., Int. Ed.* **2015**, *54*, 6506–6510.

(54) Ford, P. C. Metal Complex Strategies for Photo-Uncaging the Small Molecule Bioregulators Nitric Oxide and Carbon Monoxide. *Coord. Chem. Rev.* **2018**, *376*, 548–564.

(55) Pal, A. K.; Li, C. F.; Hanan, G. S.; Zysman-Colman, E. Blue-Emissive Cobalt(III) Complexes and Their Use in the Photocatalytic Trifluoromethylation of Polycyclic Aromatic Hydrocarbons. *Angew. Chem., Int. Ed.* **2018**, *57*, 8027–8031.

(56) Welin, E. R.; Le, C.; Arias-Rotondo, D. M.; McCusker, J. K.; MacMillan, D. W. C. Photosensitized, Energy Transfer-Mediated Organometallic Catalysis through Electronically Excited Nickel(II). *Science* **2017**, *355*, 380–384.

(57) Shields, B. J.; Kudisch, B.; Scholes, G. D.; Doyle, A. G. Long-Lived Charge-Transfer States of Nickel(II) Aryl Halide Complexes Facilitate Bimolecular Photoinduced Electron Transfer. *J. Am. Chem. Soc.* **2018**, *140*, 3035–3039.

(58) Grübel, M.; Bosque, I.; Altmann, P. J.; Bach, T.; Hess, C. R. Redox and Photocatalytic Properties of a Ni<sup>II</sup> Complex with a Macrocyclic Biquinazoline (MabiQ) Ligand. *Chem. Sci.* **2018**, *9*, 3313–3317.

(59) Zhang, Y.; Lee, T. S.; Petersen, J. L.; Milsman, C. A Zirconium Photosensitizer with a Long-Lived Excited State: Mechanistic Insight into Photoinduced Single-Electron Transfer. *J. Am. Chem. Soc.* **2018**, *140*, 5934–5947.

(60) Zhang, Y.; Petersen, J. L.; Milsman, C. Photochemical C-C Bond Formation in Luminescent Zirconium Complexes with CNN Pincer Ligands. *Organometallics* **2018**, *37*, 4488–4499.

(61) Yeung, K. T.; To, W. P.; Sun, C. Y.; Cheng, G.; Ma, C. S.; Tong, G. S. M.; Yang, C.; Che, C. M. Luminescent Tungsten(VI) Complexes: Photophysics and Applicability to Organic Light-Emitting Diodes and Photocatalysis. *Angew. Chem., Int. Ed.* **2017**, *56*, 133–137.

(62) Rudshiteyn, B.; Vibbert, H. B.; May, R.; Wesserman, E.; Warnke, I.; Hopkins, M. D.; Batista, V. S. Thermodynamic and Structural Factors That Influence the Redox Potentials of Tungsten-Alkylidyne Complexes. *ACS Catal.* **2017**, *7*, 6134–6143.

(63) Kvapilova, H.; Sattler, W.; Sattler, A.; Sazanovich, I. V.; Clark, I. P.; Towrie, M.; Gray, H. B.; Zalis, S.; Vlcek, A. Electronic Excited States of Tungsten(0) Arylisocyanides. *Inorg. Chem.* **2015**, *54*, 8518–8528.

(64) Qiao, Y. S.; Schelter, E. J. Lanthanide Photocatalysis. *Acc. Chem. Res.* **2018**, *51*, 2926–2936.

(65) Romero, N. A.; Nicewicz, D. A. Organic Photoredox Catalysis. *Chem. Rev.* **2016**, *116*, 10075–10166.

(66) Ghosh, I.; Marzo, L.; Das, A.; Shaikh, R.; König, B. Visible Light Mediated Photoredox Catalytic Arylation Reactions. *Acc. Chem. Res.* **2016**, *49*, 1566–1577.

(67) Speckmeier, E.; Fischer, T. G.; Zeitler, K. A Toolbox Approach to Construct Broadly Applicable Metal-Free Catalysts for Photoredox Chemistry: Deliberate Tuning of Redox Potentials and Importance of Halogens in Donor-Acceptor Cyanoarenes. *J. Am. Chem. Soc.* **2018**, *140*, 15353–15365.

(68) Fischer, C.; Sparr, C. Direct Transformation of Esters into Heterocyclic Fluorophores. *Angew. Chem., Int. Ed.* **2018**, *57*, 2436–2440.

(69) McCarthy, B. G.; Pearson, R. M.; Lim, C. H.; Sartor, S. M.; Damrauer, N. H.; Miyake, G. M. Structure-Property Relationships for Tailoring Phenoxazines as Reducing Photoredox Catalysts. *J. Am. Chem. Soc.* **2018**, *140*, 5088–5101.

(70) Drance, M. J.; Sears, J. D.; Mrse, A. M.; Moore, C. E.; Rheingold, A. L.; Neidig, M. L.; Figueroa, J. S. Terminal Coordination of Diatomic Boron Monofluoride to Iron. *Science* **2019**, *363*, 1203–1205.

(71) Margulieux, G. W.; Weidemann, N.; Lacy, D. C.; Moore, C. E.; Rheingold, A. L.; Figueroa, J. S. Isocyanide Analogues of Co(CO)<sub>4</sub>: A Tetraisocyanide of Cobalt Isolated in Three States of Charge. *J. Am. Chem. Soc.* **2010**, *132*, 5033–5035.

(72) Angelici, R. J.; Quick, M. H.; Kraus, G. A.; Plummer, D. T. Synthesis of Chelating Bidentate Isocyanide and Cyano Ligands and Their Metal Complexes. *Inorg. Chem.* **1982**, *21*, 2178–2184.

(73) Plummer, D. T.; Angelici, R. J. Synthesis and Characterization of Homoleptic Complexes of the Chelating Bidentate Isocyanide Ligand *tert*-BuDiNC. *Inorg. Chem.* **1983**, *22*, 4063–4070.

(74) Plummer, D. T.; Kraus, G. A.; Angelici, R. J. Synthesis of Chelating Bidentate and Tridentate Cyano Ligands and their Complexes with Group 7 Metal Carbonyls. *Inorg. Chem.* **1983**, *22*, 3492–3497.

(75) Hahn, F. E.; Tamm, M. Chelate Complexes with Triisocyanide Ligands. *Angew. Chem., Int. Ed. Engl.* **1991**, *30*, 203–205.

(76) Hahn, F. E. The Coordination Chemistry of Multidentate Isocyanide Ligands. *Angew. Chem., Int. Ed. Engl.* **1993**, *32*, 650–665.

(77) Naik, A.; Maji, T.; Reiser, O. Iron(II)-Bis(isonitrile) Complexes: Novel Catalysts in Asymmetric Transfer Hydrogenations of Aromatic and Heteroaromatic Ketones. *Chem. Commun.* **2010**, *46*, 4475–4477.

(78) Vicenzi, D.; Sgarbossa, P.; Biffis, A.; Tubaro, C.; Basato, M.; Michelin, R. A.; Lanza, A.; Nestola, F.; Bogialli, S.; Pastore, P.; Venzo, A. Platinum(II) Complexes with Novel Diisocyanide Ligands: Catalysts in Alkyne Hydroarylation. *Organometallics* **2013**, *32*, 7153–7162.

(79) Monti, F.; Baschieri, A.; Matteucci, E.; Mazzanti, A.; Sambri, L.; Barbieri, A.; Armaroli, N. A Chelating Diisocyanide Ligand for Cyclometalated Ir(III) Complexes with Strong and Tunable Luminescence. *Faraday Discuss.* **2015**, *185*, 233–248.

(80) Knorn, M.; Rawner, T.; Czerwieńiec, R.; Reiser, O. Copper-(phenanthroline)(bisisonitrile)<sup>+</sup>-Complexes for the Visible-Light-Mediated Atom Transfer Radical Addition and Allylation Reactions. *ACS Catal.* **2015**, *5*, 5186–5193.

(81) Emerich, B. M.; Moore, C. E.; Fox, B. J.; Rheingold, A. L.; Figueroa, J. S. Protecting-Group-Free Access to a Three-Coordinate Nickel(0) Tris-isocyanide. *Organometallics* **2011**, *30*, 2598–2608.

(82) Cotton, F. A.; Zingales, F. Donor-Acceptor Properties of Isonitriles as Estimated by Infrared Study. *J. Am. Chem. Soc.* **1961**, *83*, 351–355.

(83) Bohling, D. A.; Mann, K. R.; Enger, S.; Gennett, T.; Weaver, M. J.; Walton, R. A. Electrochemical Redox Behavior of the Hexakis-(arylisocyanide) Complexes of Molybdenum(0) and Tungsten(0). *Inorg. Chim. Acta* **1985**, *97*, L51–L53.

(84) Arias-Rotondo, D. M.; McCusker, J. K. The Photophysics of Photoredox Catalysis: A Roadmap for Catalyst Design. *Chem. Soc. Rev.* **2016**, *45*, 5803–5820.

(85) Bohling, D. A.; Evans, J. F.; Mann, K. R. Inductive, Steric, and Environmental Effects in the Non-Aqueous Electrochemistry of Hexakis(Aryl Isocyanide) Chromium Complexes. *Inorg. Chem.* **1982**, *21*, 3546–3551.

(86) Suzuki, K.; Kobayashi, A.; Kaneko, S.; Takehira, K.; Yoshihara, T.; Ishida, H.; Shiina, Y.; Oishi, S.; Tobita, S. Reevaluation of Absolute Luminescence Quantum Yields of Standard Solutions Using a Spectrometer with an Integrating Sphere and a Back-Thinned CCD Detector. *Phys. Chem. Chem. Phys.* **2009**, *11*, 9850–9860.



- (87) Cuttall, D. G.; Kuang, S. M.; Fanwick, P. E.; McMillin, D. R.; Walton, R. A. Simple Cu(I) Complexes with Unprecedented Excited-State Lifetimes. *J. Am. Chem. Soc.* **2002**, *124*, 6–7.
- (88) Brunner, F.; Babaei, A.; Pertegas, A.; Junquera-Hernandez, J. M.; Prescimone, A.; Constable, E. C.; Bolink, H. J.; Sessolo, M.; Orti, E.; Housecroft, C. E. Phosphane Tuning in Heteroleptic Cu(N<sup>+</sup>N)-(P<sup>+</sup>P)<sup>+</sup> Complexes for Light-Emitting Electrochemical Cells. *Dalton Trans* **2019**, *48*, 446–460.
- (89) Armaroli, N. Photoactive Mono- and Polynuclear Cu(I)-Phenanthrolines. A Viable Alternative to Ru(II)-Polypyridines? *Chem. Soc. Rev.* **2001**, *30*, 113–124.
- (90) Yoshimura, A.; Hoffman, M. Z.; Sun, H. An Evaluation of the Excited-State Absorption-Spectrum of Ru(bpy)<sub>3</sub><sup>2+</sup> in Aqueous and Acetonitrile Solutions. *J. Photochem. Photobiol., A* **1993**, *70*, 29–33.
- (91) Jarenmark, M.; Carlström, G.; Fredin, L. A.; Hedberg Wallenstein, J.; Doverbratt, I.; Abrahamsson, M.; Persson, P. Diastereomerization Dynamics of a Bistridentate Ru<sup>II</sup> Complex. *Inorg. Chem.* **2016**, *55*, 3015–3022.
- (92) Caspar, J. V.; Meyer, T. J. Application of the Energy-Gap Law to Nonradiative Excited-State Decay. *J. Phys. Chem.* **1983**, *87*, 952–957.
- (93) Klendworth, D. D.; Welters, W. W.; Walton, R. A. Redox Chemistry of Hexakis(Phenyl Isocyanide) Complexes of Molybdenum and Tungsten - The Synthesis of the 7-Coordinate Cations [M(CNPh)<sub>7</sub>]<sup>2+</sup> and their Electrochemistry and Substitution Reactions. *Organometallics* **1982**, *1*, 336–343.
- (94) Caravana, C.; Giandomenico, C. M.; Lippard, S. J. Electrochemical Studies of 7-Coordinate Isocyanide Complexes of Molybdenum(II) and Tungsten(II). *Inorg. Chem.* **1982**, *21*, 1860–1863.
- (95) Yanagisawa, S.; Ueda, K.; Taniguchi, T.; Itami, K. Potassium *t*-Butoxide Alone Can Promote the Biaryl Coupling of Electron-Deficient Nitrogen Heterocycles and Haloarenes. *Org. Lett.* **2008**, *10*, 4673–4676.
- (96) Studer, A.; Curran, D. P. Organocatalysis and C-H Activation Meet Radical- and Electron-Transfer Reactions. *Angew. Chem., Int. Ed.* **2011**, *50*, 5018–5022.
- (97) Liu, W.; Cao, H.; Zhang, H.; Zhang, H.; Chung, K. H.; He, C. A.; Wang, H. B.; Kwong, F. Y.; Lei, A. W. Organocatalysis in Cross-Coupling: DMEDA-Catalyzed Direct C-H Arylation of Unactivated Benzene. *J. Am. Chem. Soc.* **2010**, *132*, 16737–16740.
- (98) Sun, C. L.; Li, H.; Yu, D. G.; Yu, M. A.; Zhou, X. A.; Lu, X. Y.; Huang, K.; Zheng, S. F.; Li, B. J.; Shi, Z. J. An Efficient Organocatalytic Method for Constructing Biaryls through Aromatic C-H Activation. *Nat. Chem.* **2010**, *2*, 1044–1049.
- (99) Shirakawa, E.; Itoh, K.; Higashino, T.; Hayashi, T. *tert*-Butoxide-Mediated Arylation of Benzene with Aryl Halides in the Presence of a Catalytic 1,10-Phenanthroline Derivative. *J. Am. Chem. Soc.* **2010**, *132*, 15537–15539.
- (100) Zhang, L.; Yang, H.; Jiao, L. Revisiting the Radical Initiation Mechanism of the Diamine-Promoted Transition-Metal-Free Cross-Coupling Reaction. *J. Am. Chem. Soc.* **2016**, *138*, 7151–7160.
- (101) Buden, M. E.; Guastavino, J. F.; Rossi, R. A. Room-Temperature Photoinduced Direct C-H-Arylation via Base-Promoted Homolytic Aromatic Substitution. *Org. Lett.* **2013**, *15*, 1174–1177.
- (102) Zheng, X. L.; Yang, L.; Du, W. Y.; Ding, A. S.; Guo, H. Amine-Catalyzed Direct Photoarylation of Unactivated Arenes. *Chem. - Asian J.* **2014**, *9*, 439–442.
- (103) Kawamoto, T.; Sato, A.; Ryu, I. Cyanoborohydride-Promoted Radical Arylation of Benzene. *Org. Lett.* **2014**, *16*, 2111–2113.
- (104) Cheng, Y. N.; Gu, X. Y.; Li, P. X. Visible-Light Photoredox in Homolytic Aromatic Substitution: Direct Arylation of Arenes with Aryl Halides. *Org. Lett.* **2013**, *15*, 2664–2667.
- (105) Xu, Z.; Gao, L.; Wang, L. L.; Gong, M. W.; Wang, W. F.; Yuan, R. S. Visible Light Photoredox Catalyzed Biaryl Synthesis Using Nitrogen Heterocycles as Promoter. *ACS Catal.* **2015**, *5*, 45–50.
- (106) Ghosh, I.; Ghosh, T.; Bardagi, J. I.; König, B. Reduction of Aryl Halides by Consecutive Visible Light-Induced Electron Transfer Processes. *Science* **2014**, *346*, 725–728.
- (107) Pause, L.; Robert, M.; Savéant, J. M. Can Single-Electron Transfer Break an Aromatic Carbon-Heteroatom Bond in One Step? A Novel Example of Transition between Stepwise and Concerted Mechanisms in the Reduction of Aromatic Iodides. *J. Am. Chem. Soc.* **1999**, *121*, 7158–7159.
- (108) Nguyen, J. D.; D'Amato, E. M.; Narayanam, J. M. R.; Stephenson, C. R. J. Engaging Unactivated Alkyl, Alkenyl and Aryl Iodides in Visible-Light-Mediated Free Radical Reactions. *Nat. Chem.* **2012**, *4*, 854–859.
- (109) Poelma, S. O.; Burnett, G. L.; Discekici, E. H.; Mattson, K. M.; Treat, N. J.; Luo, Y. D.; Hudson, Z. M.; Shankel, S. L.; Clark, P. G.; Kramer, J. W.; Hawker, C. J.; Read de Alaniz, J. Chemoselective Radical Dehalogenation and C-C Bond Formation on Aryl Halide Substrates Using Organic Photoredox Catalysts. *J. Org. Chem.* **2016**, *81*, 7155–7160.
- (110) Kim, H.; Lee, C. Visible-Light-Induced Photocatalytic Reductive Transformations of Organohalides. *Angew. Chem., Int. Ed.* **2012**, *51*, 12303–12306.
- (111) Shon, J.-H.; Sittel, S.; Teets, T. S. Synthesis and Characterization of Strong Cyclometalating Iridium Photoreductants for Application in Photocatalytic Aryl Bromide Hydrodebromination. *ACS Catal.* **2019**, *9*, 8646–8658.
- (112) Devery, J. J.; Nguyen, J. D.; Dai, C. H.; Stephenson, C. R. J. Light-Mediated Reductive Debromination of Unactivated Alkyl and Aryl Bromides. *ACS Catal.* **2016**, *6*, 5962–5967.
- (113) Yin, H. L.; Carroll, P. J.; Manor, B. C.; Anna, J. M.; Schelter, E. J. Cerium Photosensitizers: Structure-Function Relationships and Applications in Photocatalytic Aryl Coupling Reactions. *J. Am. Chem. Soc.* **2016**, *138*, 5984–5993.
- (114) Ghosh, I.; König, B. Chromoselective Photocatalysis: Controlled Bond Activation through Light-Color Regulation of Redox Potentials. *Angew. Chem., Int. Ed.* **2016**, *55*, 7676–7679.
- (115) Neumeier, M.; Sampedro, D.; Májek, M.; de la Peña O'Shea, V. A.; Jacobi von Wangelin, A.; Pérez-Ruiz, R. Dichromatic Photocatalytic Substitutions of Aryl Halides with a Small Organic Dye. *Chem. - Eur. J.* **2018**, *24*, 105–108.
- (116) Gritter, R. J.; Chriss, R. J. Free-Radical Reactions of Pyrroles. *J. Org. Chem.* **1964**, *29*, 1163–1167.
- (117) Wenger, O. S. Photoactive Complexes with Earth-Abundant Metals. *J. Am. Chem. Soc.* **2018**, *140*, 13522–13533.